PHYSICAL REVIEW C **93**, 064326 (2016)

High-resolution study of Gamow-Teller transitions in the ^{48}Ti(^{3}He ,t)^{48}V reaction

E. Ganioğlu,[1,*] H. Fujita,[2] B. Rubio,[3] Y. Fujita,[2,4] T. Adachi,[2] A. Algora,[3,5] M. Csatlós,[5] J. M. Deaven,[6,7,8] E. Estevez-Aguado,[3] C. J. Guess,[6,7,8,†] J. Gulyás,[5] K. Hatanaka,[2] K. Hirota,[2] M. Honma,[9] D. Ishikawa,[2] A. Krasznahorkay,[5] H. Matsubara,[2,‡] R. Meharchand,[6,7,8,§] F. Molina,[3,‖] H. Okamura,[2,¶] H. J. Ong,[2] T. Otsuka,[10] G. Perdikakis,[6,11] C. Scholl,[12,**] Y. Shimbara,[13] G. Susoy,[1] T. Suzuki,[2] A. Tamii,[2] J. H. Thies,[14,††] R. G. T. Zegers,[6,7,8] and J. Zenihiro[2,‡‡]

[1]*Department of Physics, Istanbul University, Istanbul 34134, Turkey*
[2]*Research Center for Nuclear Physics, Osaka University, Ibaraki, Osaka 567-0047, Japan*
[3]*Instituto de Física Corpuscular, CSIC-Universidad de Valencia, E-46071 Valencia, Spain*
[4]*Department of Physics, Osaka University, Toyonaka, Osaka 560-0043, Japan*
[5]*Institute of Nuclear Research (ATOMKI), H-4001 Debrecen, Post Office Box 51, Hungary*
[6]*National Superconducting Cyclotron Laboratory, Michigan State University, East Lansing, Michigan 48824-1321, USA*
[7]*Joint Institute for Nuclear Astrophysics, Michigan State University, East Lansing, Michigan 48824, USA*
[8]*Department of Physics and Astronomy, Michigan State University, East Lansing, Michigan 48824, USA*
[9]*Center for Mathematical Science, University of Aizu, Aizu-Wakamatsu, Fukushima 965-8580, Japan*
[10]*Department of Physics, University of Tokyo, Hongo, Bunkyo, Tokyo 113-0033, Japan*
[11]*Department of Physics, Central Michigan University, Mt. Pleasant, MI 48859, USA*
[12]*Institut für Kernphysik, Universität zu Köln, 50937 Köln, Germany*
[13]*CYRIC, Tohoku University, Aramaki, Aoba, Sendai, 980-8578, Japan*
[14]*Institut für Kernphysik, Westfälische Wilhelms-Universität, D-48149 Münster, Germany*

(Received 28 April 2016; published 30 June 2016)

In this work we have studied $T_z = +2 \rightarrow +1$, Gamow-Teller (GT) transitions in the ^{48}Ti(^{3}He ,t)^{48}V charge-exchange reaction at 140 MeV/nucleon and 0° at the Research Center for Nuclear Physics, Osaka. From the high-resolution facility, consisting of a high-dispersion beamline and the Grand Raiden spectrometer, the spectrum had an energy resolution of 21 keV, among the best achieved. Individual GT transitions were observed and GT strength was derived for each state populated up to an excitation energy of 12 MeV. The total sum of the B(GT) strength observed in discrete states was 4.0, which is 33% of the sum-rule-limit value of 12. The results were compared with the results of shell-model calculations carried out with the GXPF1J interaction. The measured B(GT) distribution was also compared with that obtained in the (^{3}He,t) charge-exchange reaction on ^{47}Ti. On the assumption of isospin symmetry the β spectrum of the $T_z = -2$ nucleus ^{48}Fe was deduced from the observed spectrum in the ^{48}Ti(^{3}He ,t)^{48}V reaction and this predicted spectrum was compared with the measured one.

DOI: 10.1103/PhysRevC.93.064326

I. INTRODUCTION

The nucleus ^{48}V is located close to the middle of the $f_{7/2}$ shell. In the present work, we report the results of high-resolution studies of the ^{48}Ti(^{3}He ,t)^{48}V reaction carried out at 140 MeV/nucleon. It is part of systematic studies of (^{3}He,t) reactions on the five stable titanium isotopes with masses $A = 46$–50. In turn this is part of a wider program to examine how the Gamow-Teller (GT) strength distributions change as we move through the fp shell in both N and Z.

Charge-exchange (CE) reactions and β decay are complementary processes. The latter provides the most direct information on the GT transition strength, B(GT). The information obtained, however, is limited to transitions to states with excitation energies (E_x) in the daughter nucleus that are allowed by the β-decay Q value. Moreover the feeding to higher excited states decreases rapidly because of the rapidly decreasing phase-space factor. In CE reactions one can observe GT transitions to states at high excitation energies since there is no Q-value limitation (e.g., see Refs. [1–5]). In CE reactions at intermediate bombarding energies ∼100 MeV/nucleon and forward angles close to 0°, there is a close proportionality for GT transitions between the differential cross sections and the B(GT) values [6,7],

$$\frac{d\sigma_{\mathrm{GT}}}{d\Omega}(q,\omega) \simeq K(\omega) N_{\sigma\tau} |J_{\sigma\tau}(q)|^2 B(\mathrm{GT}) \quad (1)$$

$$= \hat{\sigma}_{\mathrm{GT}} F(q,\omega) B(\mathrm{GT}), \quad (2)$$

where $J_{\sigma\tau}(q)$ is the volume integral of the effective interaction $V_{\sigma\tau}$, $K(\omega)$ is the kinematic factor, ω is the total energy

*ganioglu@istanbul.edu.tr
†Present address: Department of Physics and Astronomy, Swarthmore College, Swarthmore, Pennsylvania 19081, USA.
‡Present address: Tokyo Women's Medical University, Tokyo 162-8666, Japan.
§Present address: Institute for Defense Analyses, Alexandria, Virginia 22206, USA.
‖Present address: Comisión Chilena de Energía Nuclear, Post Office Box 188-D, Santiago, Chile.
¶Deceased.
**Present address: Institute for Work Design of North Rhine-Westphalia, Radiation Protection Services, 40225 Dusseldorf, Germany.
††Present address: FH Bielefeld - University of Applied Sciences, 32427 Minden, Germany.
‡‡Present address: RIKEN Nishina Center, Wako, Saitama 351-0198, Japan.

transfer, and $N_{\sigma\tau}$ is a distortion factor. The value $\hat{\sigma}_{\mathrm{GT}}$ is the GT unit cross section for a specific nuclear mass A at a given incoming energy, and the value $F(q,\omega)$ gives the dependence of the GT cross sections on the momentum and energy transfers. It has a value of unity at $q = \omega = 0$ and changes smoothly as a function of E_x. It can be reliably obtained from distorted-wave Born approximation (DWBA) calculations.

In the 1980s, studies of (p,n) reactions at intermediate energies became possible and B(GT) distributions were studied for various nuclei [2]. It was found that broad resonance structures in GT strengths appear systematically at $E_x \approx 10$ MeV. In general these GT resonances (GTRs) cannot be observed in β decay because of the constraints imposed by the β-decay Q value. Despite the success of these (p,n) reaction studies they were limited by the achievable energy resolutions, which were in excess of 300 keV. As a result it was difficult to resolve close-lying, individual peaks in the spectra even if the level density was not very high. More recently this constraint was overcome by using other CE reactions such as the $(^3\mathrm{He},t)$ reaction at intermediate incident energies $\geqslant$100 MeV/nucleon [4]. Precise beam matching techniques [8] with the beamline and magnetic spectrometer system at the Research Center for Nuclear Physics (RCNP) [9], Osaka, routinely allow one to produce spectra with an energy resolution of $\leqslant$30 keV for incident beam energies of 140 MeV/nucleon at 0°. This allows one to observe discrete transitions to states not just at low excitation energies but also in the region of the GTR at $\approx$10 MeV [10–15].

The close proportionality given in Eq. (2) has been examined for the $(^3\mathrm{He},t)$ measurements by comparing the B(GT) values for analogous transitions in the CE reaction and the corresponding β decays of the mirror nuclei in the *sd* shell. In general, with some exceptions, the proportionality was good to within $\approx$5% for transitions assigned $\Delta L = 0$ in studies of the mass $A = 23$, 26, 27, and 34 systems [4,11–14]. These observations have now been followed by studies of the strengths of GT transitions in $(^3\mathrm{He},t)$ reactions on the $T_z = +1$, $f_{7/2}$-shell nuclei ^{42}Ca, ^{46}Ti, ^{50}Cr, and ^{54}Fe at RCNP. The results were compared with the GT strengths measured in the β decays of the equivalent $T_z = -1$ nuclei ^{42}Ti, ^{46}Cr, ^{50}Fe, and ^{54}Ni [16]. The comparison of the B(GT) values obtained for the analogous GT transitions in CE and β decay in the $f_{7/2}$ shell confirms the earlier observations that the proportionality in Eq. (2) holds for strong but not necessarily for weak transitions [17].

Recently these studies were extended to measurements of the GT transitions from the $T_z = +3/2$ nucleus ^{47}Ti to states in the $T_z = +1/2$ nucleus ^{47}V [15]. Here we report on a further extension to measurements of the $(^3\mathrm{He},t)$ reaction on the $T_z = +2$ nucleus ^{48}Ti leading to states in $T_z = +1$ ^{48}V. The results obtained are compared with similar measurements for ^{47}Ti$(^3\mathrm{He},t)^{47}$V and with the results of shell-model calculations.

II. EXPERIMENT

The ^{48}Ti$(^3\mathrm{He},t)^{48}$V reaction has been studied at RCNP, Osaka, with the high-resolution facility and a high-quality beam of 140 MeV/nucleon from the $K = 400$ ring cyclotron [9]. This facility combines a high-dispersion beamline WS course [18] with the Grand Raiden spectrometer [19]. The ^{3}He beam was stopped in a Faraday cup placed inside the first dipole magnet. The self-supporting ^{48}Ti target that was used has an enrichment of 99.1% and an areal density of 0.85 mg/cm^2. The beam current was typically 21 pnA and the spectra were recorded over a period of an hour. The outgoing tritons were momentum analyzed within the full acceptance of the spectrometer and detected at the focal plane with a system consisting of two multiwire drift chambers (MWDCs) that allow track reconstruction [20] and two plastic scintillators used both for the creation of triggers to start the data acquisition system and for particle identification. The use of matching techniques [8] and the *faint beam method* [21,22] resulted in a measured energy resolution of 21 keV. This meant that we were able to resolve individual states in ^{48}V up to $E_x = 12.5$ MeV. Figure 1(a) shows the 0° spectrum from the ^{48}Ti target with scattering angles $\Theta \leqslant 0.5°$, where Θ is defined by $\Theta_{\mathrm{lab}} = \arctan\sqrt{\tan\theta^2 + \tan\phi^2}$ at angles near 0°, and θ and ϕ are the scattering angles in the x and y directions. It is important to determine the scattering angle Θ accurately near 0°, hence it is necessary to measure θ and ϕ equally well. Good θ resolution was achieved by using the *angular dispersion matching* technique [8], while good ϕ resolution was achieved by applying the *over-focus mode* of the Grand Raiden spectrometer [23]. A more detailed description of the experimental procedure can be found in Ref. [24].

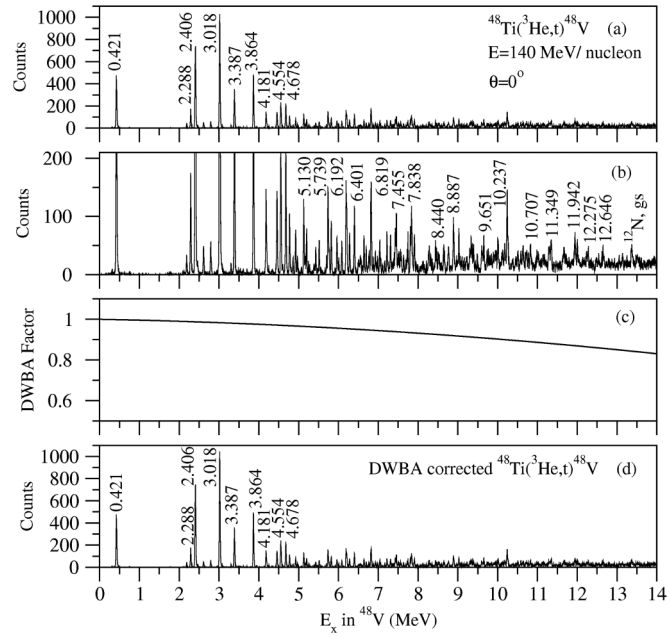

FIG. 1. (a) The ^{48}Ti$(^3\mathrm{He},t)^{48}$V spectrum at 0°. Events with scattering angles $\Theta \leqslant 0.5°$ are included. States prominently populated by $\Delta L = 0$ transitions are indicated by their excitation energies. (b) The same spectrum is shown with the scale on the y axis expanded by a factor of $\approx$ 4.5. (c) The correction factor for the gradual decrease in $F(q,\omega)$ calculated using the results of DWBA calculations (see Sec. III) as a function of energy. (d) The spectrum shown in (a) corrected for the results of the DWBA calculations shown in (c).

The details of the spectrum can be seen better in Fig. 1(b) where the same spectrum is shown on an expanded scale. Here one can see the continuous background from quasifree scattering beginning at about the proton separation energy, $S_p \approx 6.83$ MeV [25].

III. DATA ANALYSIS

A peak decomposition program SFIT [26] was used to determine the positions of the peaks and the number of counts they contained. In order to obtain the peak positions the shape of a well-defined isolated peak at 2.288 MeV was used as a reference and particular attention was paid to the tail of the peak to get a reliable response function.

From the peak positions obtained, the E_x values of states in the higher excitation energy region were determined using the well-known E_x values of states in ^{12}N, ^{13}N, and ^{16}F as references using kinematical calculations. The states were observed in a spectrum from a thin Mylar target with an areal density of ≈ 1 mg/cm^2. The measurement was performed under the same conditions used with the ^{48}Ti target. The E_x values of the ^{48}V states could be determined by an interpolation process and they are listed in Tables I–IV. Prior to the present work the E_x values of only a few states were known [25] in ^{48}V. All of these states lie below 3.3 MeV and they are shown in Table I. In the present work most of these E_x values could be reproduced within a few keV. In addition the E_x value of the ^{12}N ground state (g.s), which appeared at ≈13.4 MeV in the ^{48}V spectrum was reproduced with an error of 5 keV. Therefore, even if we take the uncertainty of the peak decomposition process into account, we estimate that the E_x values of the states listed in Tables I–IV have an accuracy better than 10 keV up to the region around 12 MeV. Due to the high isotopic abundance (99.1%) of ^{48}V in the target, peaks from other Ti isotopes were weak in our spectrum. Above the 12 MeV region, due to the high level density, the separation of peaks was difficult, even with the experimental energy resolution of 21 keV.

A continuous background was observed above the proton separation energy $S_p \approx 6.83$ MeV. It increased with increasing excitation energy but it was essentially saturated at $E_x \approx$ 11.5 MeV. Accordingly, a smooth background was subtracted empirically in the peak fit analysis. In order to identify $\Delta L = 0$ transitions, the relative intensities of the peaks in the angle cuts $\theta = 0°$–$0.5°$, $0.5°$–$0.8°$, $0.8°$–$1.2°$, $1.2°$–$1.6°$, and $1.6°$–$2.0°$ were examined. Figure 2 shows examples of the angular distributions, normalized to the counts at 0°, for some of the stronger transitions leading to states at low E_x. The transition to the state at 2.406 MeV was used as a standard $\Delta L = 0$ transition since the state populated has spin and parity 1^+. With the exception of the transition to the 2.465 MeV state it is clear that there is no clear enhancement at the larger scattering angles. This confirms that all of the other transitions in the $0°$–$0.5°$ degree cut shown in Fig. 2 have $\Delta L = 0$ character. More generally, in the low-lying region of excitation energy, where the transitions and the states are fairly well separated, the ΔL values were well determined. The comparison of the angular distributions of all of the transitions in Fig. 1 indicate that most of the strong transitions have $\Delta L = 0$ character.

TABLE I. States observed in the ^{48}Ti(^{3}He ,t)^{48}V reaction up to $E_x = 6.6$ MeV. The B(GT) values for weakly populated states with $\Delta L = 0$ are listed in two categories marked by S and SS, where S indicates $0.005 < B(\mathrm{GT}) < 0.01$ and SS indicates $B(\mathrm{GT}) \leqslant 0.005$. For these states the numbers of counts observed in the $\Theta \leqslant 0.5°$ spectrum are listed.

Evaluated values[a]		(^{3}He ,t)[b]			
E_x^c (MeV)	J^π	E_x (MeV)	ΔL	Counts	B(GT)[d]
0.421	1^+	0.421	0	3410(81)	0.224(13)
		2.186	0	197(19)	0.013(1)
2.289	1^+	2.288	0	1140(47)	0.076(5)
2.408 (7)	1^+	2.406	0	5260(100)	0.351(19)
		2.465	$\geqslant 1$	137(20)	
		2.611	0	333(25)	0.022(2)
		2.792	0	356(28)	0.024(2)
3.019	$(0)^+$	3.018 [e]	0	7260(117)	
		3.387	0	2180(65)	0.147(9)
3.866	1^+	3.864	0	3140(76)	0.213(12)
		3.945	0	64(12)	SS
		4.181	0	821(59)	0.056(5)
		4.201	(0)	201(43)	0.014(3)
		4.245	0	53(11)	SS
		4.456	0	1030(44)	0.070(5)
		4.554	0	1480(52)	0.101(6)
		4.595	0	80(14)	SS
		4.678	0	1560(55)	0.107(7)
		4.773	0	694(36)	0.048(3)
		4.857	0	172(18)	0.012(1)
		4.924	0	471(30)	0.032(3)
		4.971	0	195(20)	0.013(2)
		5.067	0	64(12)	SS
		5.130	0	830(42)	0.057(4)
		5.164	0	166(27)	0.011(2)
		5.199	0	436(31)	0.030(3)
		5.246	(0)	61(15)	SS
		5.277	0	80(15)	S
		5.388	0	117(16)	S
		5.430	0	273(24)	0.019(2)
		5.477	$\geqslant 1$	43(12)	
		5.516	$\geqslant 1$	312(24)	
		5.567	0	50(11)	SS
		5.702	0	125(20)	S
		5.739	0	956(52)	0.067(5)
		5.766	0	226(33)	0.016(2)
		5.820	0	597(33)	0.042(3)
		5.913	$\geqslant 1$	54(11)	
		5.965	0	474(31)	0.033(3)
		6.005	0	125(16)	S
		6.085	$\geqslant 1$	387(27)	
		6.192	0	911(80)	0.064(7)
		6.208	0	574(70)	0.040(5)
		6.280	0	456(29)	0.032(3)
		6.401	0	847(40)	0.060(4)
		6.464	0	45(11)	SS
		6.501	0	134(50)	S
		6.516	(0)	114(49)	S

TABLE I. (*Continued.*)

Evaluated values[a]		(^{3}He ,t)[b]			
E_x^c (MeV)	J^π	E_x (MeV)	ΔL	Counts	B(GT)[d]
		6.548	0	192(39)	0.014(3)
		6.568	(0)	127(32)	S

[a]Taken from the compilation in Ref. [25].
[b]Present work.
[c]Energy uncertainties of < 1 keV are not indicated.
[d]From R^2 evaluation.
[e]The IAS.

This is indicated in Tables I–IV. However, at higher excitation energies, where the level density is high, the determination of the ΔL values became difficult. A clear enhancement at larger angles was observed for some of the weaker transitions. This identifies them as having $\Delta L \geqslant 1$. When the determination is uncertain, the states are assigned $\Delta L = 0$ in brackets in the tables. Where the transitions have been assigned $\Delta L = 0$ character, we assume that they are GT transitions, except for the transition to the Isobaric Analog State (IAS) [4]. For details of the analysis of the angular distributions, see Refs. [27,28].

Transitions to individual states were observed up to 12.67 MeV in the ^{48}Ti(^{3}He ,t) reaction. The relative B(GT) values for these transitions were derived by applying the proportionality given by Eq. (2) to the measured intensity of each peak. The gradual decrease in $F(q,\omega)$ as a function of excitation energy was corrected by using the results of distorted-wave Born approximation calculations. For this purpose, the DW81 code [29] was used where it was assumed that the transitions were between the $\nu f_{7/2} \rightarrow \pi f_{7/2}$ and $\nu f_{7/2} \rightarrow \pi f_{5/2}$ configurations. In the calculations we followed the procedure described in Refs. [30–32].

The optical potential parameters were taken from Ref. [33]. The DWBA calculation indicated that the GT cross section decreases with increasing excitation energy, and the decrease was $\approx$7% from the g.s to $E_x = 8$ MeV. To obtain absolute B(GT) values, we used the R^2 value defined by the ratio of the GT and Fermi unit cross sections

$$R^2 = \frac{\hat{\sigma}_{\rm GT}(0^\circ)}{\hat{\sigma}_{\rm F}(0^\circ)} = \frac{\sigma_{\rm GT}(0^\circ)}{B({\rm GT})} \Big/ \frac{\sigma_{\rm F}(0^\circ)}{B({\rm F})}. \quad (3)$$

If the R^2 value is known for a mass A system, the B(GT) value of the transition to a given state can be deduced from the DWBA corrected 0° cross sections of the state and the IAS where we assume that all of the Fermi transition strength is concentrated in the transition to the IAS at 3.018 MeV and that it takes the value of $B(\mathrm{F}) = N - Z = 4$, the complete sum rule value. In addition we assume that R^2 is a smooth function of A. The A dependence of R^2 has been systematically studied and a smooth increase in R^2 was observed with increasing A [34,35]. A value of $R^2 = 8.2(4)$ can be deduced for the $A = 48$ nuclei by quadratically interpolating the experimental R^2 values obtained for $A = 26$ [12], 34 [14], 46 [36], 54 [24], 64 [37], 78 [38], 118, and 120 [39]. The B(GT) values were derived for all states assigned to have $\Delta L = 0$ and they are listed in Tables I–IV.

TABLE II. States observed in the ^{48}Ti(^{3}He ,t)^{48}V reaction between $E_x = 6.6$ and 8.6 MeV. For details, see the caption to Table I.

(^{3}He ,t)[a]			
E_x (MeV)	ΔL	Counts	B(GT)
6.603	(0)	79(16)	S
6.641	0	438(29)	0.031(3)
6.697	0	305(25)	0.022(2)
6.748	$\geqslant$1	81(40)	
6.770	0	248(42)	0.018(3)
6.819	0	1310(52)	0.093(6)
6.874	0	169(21)	0.012(2)
6.924	0	263(28)	0.019(2)
6.950	0	73(21)	SS
6.982	0	195(23)	0.014(2)
7.038	0	347(32)	0.025(3)
7.061	0	98(21)	S
7.106	0	101(16)	S
7.163	0	131(18)	S
7.219	0	420(33)	0.030(3)
7.247	$\geqslant$1	72(20)	
7.308	0	458(32)	0.033(3)
7.350	($\geqslant$1)	85(27)	
7.374	0	99(37)	S
7.398	0	149(37)	0.011(3)
7.428	0	435(45)	0.031(4)
7.455	0	696(46)	0.050(4)
7.496	0	144(32)	0.010(2)
7.520	0	214(30)	0.015(2)
7.558	0	241(35)	0.017(3)
7.580	0	155(30)	0.011(2)
7.639	0	207(22)	0.015(2)
7.693	0	117(21)	S
7.728	0	203(44)	0.015(3)
7.749	0	260(44)	0.019(3)
7.810	0	514(43)	0.037(4)
7.838	0	727(66)	0.052(5)
7.862	$\geqslant$1	85(40)	
7.909	0	475(34)	0.034(3)
7.955	($\geqslant$1)	100(19)	
7.990	(0)	77(16)	S
8.049	0	65(16)	SS
8.086	0	85(19)	S
8.119	(0)	132(22)	0.010(2)
8.161	0	72(16)	SS
8.216	(0)	80(16)	S
8.262	0	137(47)	0.010(3)
8.279	0	297(49)	0.022(4)
8.316	0	176(25)	0.013(2)
8.353	0	99(19)	S
8.401	(0)	82(18)	S
8.440	0	317(37)	0.023(3)
8.465	0	188(33)	0.014(2)
8.505	0	211(32)	0.015(2)
8.530	(0)	189(31)	0.014(2)
8.572	(0)	91(21)	S
8.600	(0)	55(19)	SS

[a]Present work.

TABLE III. States observed in the ^{48}Ti(^{3}He ,t)^{48}V reaction between $E_x = 8.6$ and 10.7 MeV. For details, see the caption to Table I.

(^{3}He ,t)[a]			
E_x (MeV)	ΔL	Counts	B(GT)
8.645	0	304(42)	0.022(3)
8.666	(0)	129(35)	S
8.744	(0)	106(29)	S
8.767	0	312(36)	0.023(3)
8.821	$\geqslant$1	73(17)	
8.887	0	543(80)	0.040(6)
8.904	(0)	227(73)	0.017(5)
8.967	0	142(26)	0.010(2)
8.998	(0)	120(29)	S
9.027	0	429(37)	0.032(3)
9.061	0	132(24)	0.010(2)
9.105	0	171(24)	0.013(2)
9.157	(0)	111(58)	S
9.198	(0)	74(36)	S
9.220	0	115(73)	S
9.232	0	103(63)	S
9.268	($\geqslant$1)	52(19)	
9.301	0	287(34)	0.021(3)
9.333	0	378(39)	0.028(3)
9.362	$\geqslant$1	261(34)	
9.397	0	286(30)	0.021(3)
9.446	0	98(20)	S
9.492	0	183(21)	0.014(2)
9.606	0	340(32)	0.025(3)
9.651	(0)	440(34)	0.033(3)
9.699	$\geqslant$1	52(18)	
9.732	0	223(27)	0.017(2)
9.770	0	212(28)	0.016(2)
9.808	0	149(26)	0.011(2)
9.846	0	188(25)	0.014(2)
9.891	0	200(27)	0.015(2)
9.930	0	244(32)	0.018(3)
9.962	0	252(31)	0.019(3)
10.008	0	431(38)	0.033(3)
10.038	$\geqslant$1	64(22)	
10.073	(0)	86(21)	S
10.107	0	183(33)	0.014(3)
10.133	0	222(35)	0.017(3)
10.179	$\geqslant$1	366(33)	
10.237	0	834(56)	0.063(5)
10.258	(0)	287(48)	0.022(4)
10.286	$\geqslant$1	58(25)	
10.334	0	91(21)	S
10.373	0	136(24)	0.010(2)
10.446	(0)	91(31)	S
10.470	0	129(32)	0.010(2)
10.509	0	227(28)	0.017(2)
10.564	0	108(36)	S
10.585	0	198(39)	0.015(3)
10.626	0	252(39)	0.019(3)
10.653	$\geqslant$1	140(35)	
10.707	0	238(33)	0.018(3)

[a]Present work.

TABLE IV. States observed in the ^{48}Ti(^{3}He ,t)^{48}V reaction between $E_x = 10.7$ and 12.7 MeV. For details, see the caption to Table I.

(^{3}He ,t)[a]			
E_x (MeV)	ΔL	Counts	B(GT)
10.735	0	183(31)	0.014(3)
10.777	0	156(25)	0.012(2)
10.823	0	293(33)	0.023(3)
10.856	$\geqslant$1	117(26)	
10.901	$\geqslant$1	61(19)	
10.955	$\geqslant$1	77(20)	
10.984	(0)	171(29)	0.013(2)
11.017	0	215(29)	0.017(2)
11.061	(0)	103(23)	S
11.102	(0)	97(23)	S
11.139	0	177(28)	0.014(2)
11.174	0	161(27)	0.013(2)
11.207	$\geqslant$1	94(23)	
11.280	(0)	206(37)	0.016(3)
11.302	0	238(41)	0.019(3)
11.335	0	198(69)	0.015(5)
11.349	0	297(65)	0.023(5)
11.419	$\geqslant$1	65(20)	
11.466	$\geqslant$1	79(21)	
11.512	$\geqslant$1	57(20)	
11.565	$\geqslant$1	58(20)	
11.636	0	151(28)	0.012(2)
11.669	0	258(33)	0.020(3)
11.707	$\geqslant$1	143(26)	
11.768	$\geqslant$1	72(25)	
11.794	$\geqslant$1	72(24)	
11.858	$\geqslant$1	78(25)	
11.883	$\geqslant$1	62(27)	
11.942	0	684(70)	0.054(6)
11.991	(0)	136(56)	0.011(4)
12.008	(0)	216(55)	0.017(4)
12.046	(0)	107(25)	S
12.133	(0)	93(24)	S
12.169	(0)	101(24)	S
12.233	(0)	226(30)	0.018(3)
12.275	0	254(30)	0.020(3)
12.321	$\geqslant$1	53(24)	
12.346	0	63(24)	SS
12.398	(0)	54(21)	SS
12.482	0	121(26)	0.010(2)
12.538	0	106(32)	S
12.618	$\geqslant$1	102(31)	
12.646	(0)	220(41)	0.018(3)
12.675	$\geqslant$1	90(29)	

[a]Present work.

The B(GT) values of weakly excited states with $0.005 < B(\mathrm{GT}) < 0.01$ are marked by the sign "S" and those with $B(\mathrm{GT}) \leqslant 0.005$ as "SS" in Tables I–IV. The uncertainties in the B(GT) values given in Tables I–IV include the statistical uncertainties in the experimental data, the quality of the peak-fit analysis, and the uncertainty in R^2. However, the uncertainties associated with the background subtraction were

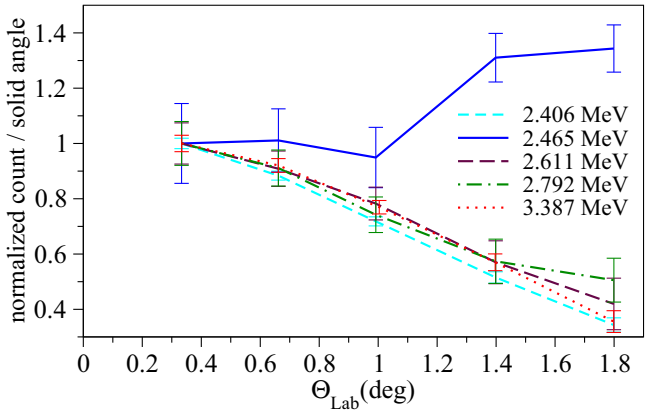

FIG. 2. Angular distributions for selected transitions. They are labeled by the excitation energy of the level populated in the CE reaction. In this figure we have chosen a few weak transitions to show the power of the method to identify $\Delta L = 0$ transitions (see text). The counts at each angle are normalized to unity at $\Theta = 0^\circ$–0.5°.

not included. Therefore, the B(GT) values of the transitions to the states in the region at higher energy, where the background counts were larger, can have larger uncertainties.

For the states assigned to have $\Delta L \geqslant 1$, counts in $\Theta \leqslant 0.5^\circ$ are listed to show the intensities.

IV. RESULTS AND DISCUSSION

A. B(GT) distribution in ^{48}V

The B(GT) distribution obtained for the ^{48}Ti(^{3}He ,t)^{48}V reaction is shown in Fig. 3(a). Note that the B(GT) distribution

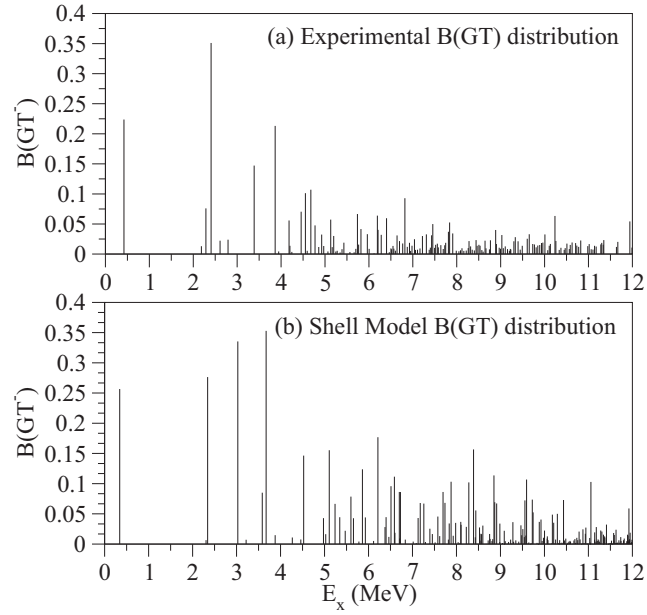

FIG. 3. Comparison of (a) the measured B(GT) strength distribution and (b) shell-model calculations with the GXPF1J interaction of the B(GT) strength distribution for the ^{48}Ti(^{3}He ,t)^{48}V reaction (see text).

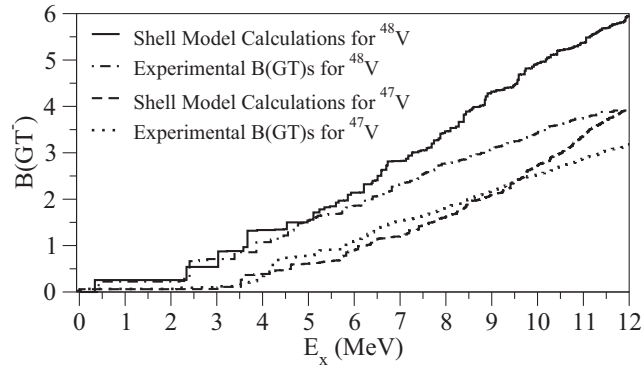

FIG. 4. Comparison of the accumulated experimental and theoretical (shell model) B(GT) distributions for both the ^{48}Ti(^{3}He ,t)^{48}V reaction measured in the present work and the ^{47}Ti(^{3}He ,t)^{47}V reaction measured earlier [15].

is shown up to 12 MeV in the figures although the states in Table IV are listed up to 12.7 MeV. The B(GT) distribution shows that the GT strength is highly fragmented and distributed over many discrete states. However, no compact structure corresponding to the GT resonance was observed.

Shell-model (SM) calculations were performed using the GXPF1J interaction [40,41]. The model space was restricted to the pf shell and an inert ^{40}Ca core was assumed. The theoretical B(GT) values for this reaction include the average normalization factor (the so-called quenching factor) of $(0.74)^2$ [42]. The results of the SM calculations are shown in Fig. 3(b). They are in reasonable agreement with the observed B(GT) strength in the region up to ∼5 MeV. Moreover, the building up of the GTR can be seen around 9 MeV.

The difference between the measured and calculated strengths is clearly seen in Fig. 4 where the accumulated B(GT) strength is plotted as a function of excitation energy in ^{48}V up to 12 MeV. As mentioned above, up to ∼5 MeV they are in reasonable agreement. From ∼5 MeV the SM predicts greater strength than is observed. In both experiment and the SM, there is a jump in the accumulated B(GT) strength just above 2 MeV. Below this energy, the states expected are essentially due to the coupling of the odd neutron and proton in the $f_{7/2}$ orbitals.

B. Comparison of the B(GT) distributions in ^{47}V and ^{48}V

It is interesting to compare the B(GT) distribution from the ^{48}Ti(^{3}He ,t)^{48}V reaction with that observed in the ^{47}Ti(^{3}He ,t)^{47}V reaction [15]. Figure 4 shows the accumulated strengths as a function of excitation energy for the two reactions from both experiment and the SM. Comparing the $A = 47$ and $A = 48$ cases we see very similar behavior. The main difference is that the jump in the accumulated B(GT), seen both in theory and experiment, is delayed in energy by ≈2 MeV in the case of the odd nucleus ^{47}V. This can be explained in terms of the diagrams shown in Figs. 5(a)–5(c), where we are concerned with the particles and interactions between them in ^{47}V and ^{48}V. In the case of ^{48}Ti, we start with even numbers of protons and neutrons. In a GT transition one of the neutrons in a pair in the $f_{7/2}$

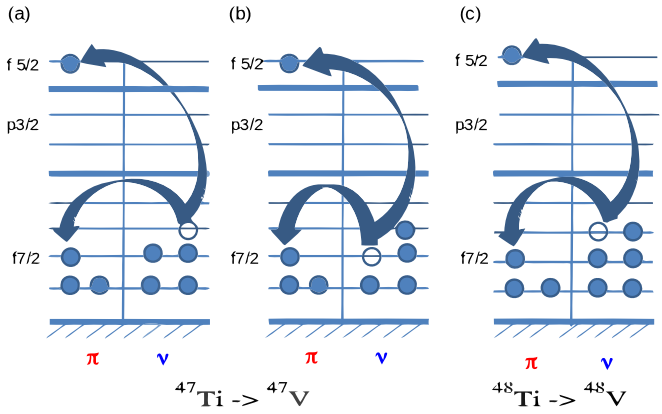

FIG. 5. Schematic picture of the transitions involved in the CE reactions on ^{47}Ti and ^{48}Ti. Full circles represent the particles in the final nucleus above $N = 20$ and $Z = 20$. Empty circles show the original position of the neutron before it is transformed into a proton. It provides a simple explanation of the differences in the accumulated B(GT) distributions seen in Fig. 4 (see text).

orbital is transformed into a proton in the ^{48}V final nucleus, hence we populate proton-neutron excitations which are the lowest possible excitations in the odd-odd nucleus ^{48}V. There are two possibilities for such GT transitions, see Fig. 5(c): (i) $\nu f_{7/2} \rightarrow \pi f_{7/2}$, which should populate states lying at low energy, and (ii) $\nu f_{7/2} \rightarrow \pi f_{5/2}$, which should populate states in ^{48}V at higher energy. Let us now turn to the $A = 47$ case. Initially we have a valence neutron in the $\nu f_{7/2}$ orbital in ^{47}Ti. This neutron can proceed by a GT transition to the $\pi f_{7/2}$ orbital, which should populate a level at very low energy close to the g.s., or to the $\pi f_{5/2}$ orbital and populate a state at higher excitation energy. Additionally in the ^{47}V case, if we think of GT transitions involving a neutron from the $(\nu f_{7/2})^2$ pairs, we have to break the pair first, which typically costs ≈2 MeV, and in the same way as in the $A = 48$ case the GT transitions lead us to the transformation of one of the neutrons from the pair into the proton in the $\pi f_{7/2}$ or the $\pi f_{5/2}$ orbitals, see Fig. 5(b). The states populated in the second case should be similar to those in the ^{48}V case adding the extra odd neutron in ^{47}V but shifted by the pairing energy of ≈2 MeV, which is what we see in Fig. 4. Since in the ^{47}V case there are four paired neutrons and one odd neutron and in the ^{48}V case there are six paired neutrons, the accumulated strength of ^{47}V up to 12 MeV should be similar to the accumulated strength in ^{48}V up to 10 MeV, to take into account the energy shift, corrected by the number of neutron pairs and the odd neutron in the $f_{7/2}$ orbital, namely, $3.5 \times 5/6 = 2.9$, which is close to the value of 3.2 observed (see Fig. 4). To verify if this effect is reproduced by the calculations, we have shifted the energy of the shell-model calculations for ^{48}Ti → ^{48}V by 2 MeV, scaled by a factor of $5/6 = 0.833$ and compared with SM calculations for ^{47}Ti → ^{47}V. The result is shown in Fig. 6(a). In the same way, we have shifted the experimental accumulated strength distribution, scaled by 0.833 and by 2 MeV and compared it with the ^{47}V distribution in Fig. 6(b). The agreement is remarkable in both cases, which gives us some confidence in our interpretation.

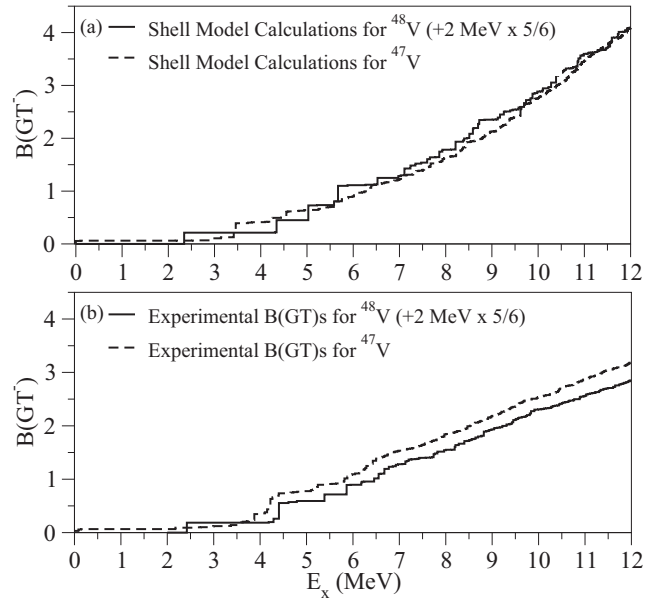

FIG. 6. (a) Comparison of the accumulated theoretical (SM) B(GT) distributions for ^{47}V and ^{48}V shifted by 2 MeV and scaled by a factor of $5/6 = 0.833$. (b) Comparison of the accumulated experimental B(GT) distributions for ^{47}V and ^{48}V obtained in the same way as in (a).

C. Total B(GT) strength

The total sum of the B(GT) strength observed in the discrete states in ^{48}V up to 12 MeV was 4.0. We suggest that this B(GT) value is the minimum of the total sum in the entire region up to 12 MeV due to background ambiguities (see discussion below). One can see that this value is only 33% of the sum-rule-limit value of $3(N - Z)$ even if the negative contribution from the GT strengths in the β^+ direction is ignored. It should be noted that the SM predicts the sum of the B(GT) strength to be 5.95 up to 12 MeV.

The continuum from quasifree scattering (QFS) [43,44] is expected to be observed above the proton separation energy of $S_p = 6.83$ MeV. Since there is no theory for reliably calculating the cross section of the QFS continuum, a background described by a smooth line was subtracted in our analysis, as mentioned earlier. Under the extreme assumption that the background counts are all due to GT transitions, this would add a value of 0.67 to the summed B(GT) value in the region up to 12 MeV. Therefore, our results show that the total sum of the B(GT) located in the energy region from 0 to 12 MeV is ≈33%, but can never be larger than 39% of the sum-rule-limit value.

D. Mirror β decay

In principle one can normalize the measured B(GT) values from CE using the measured B(GT) values from the complementary β decay of the mirror nucleus assuming isospin symmetry. In the present case this is not possible because too little is known of the decay of the $T_z = -2$ mirror nucleus ^{48}Fe. However we can use our measured relative B(GT) values in the ^{48}Ti(^{3}He,t)^{48}V CE reaction, normalized using

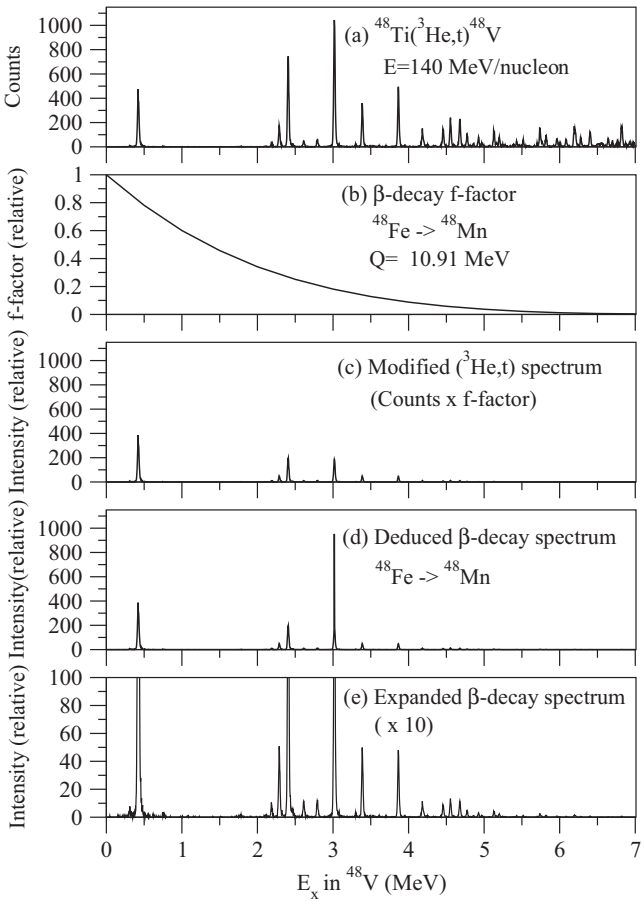

FIG. 7. (a) ^{48}Ti(^{3}He ,t)^{48}V DWBA corrected spectrum up to 7 MeV for $\Theta \leqslant 0.5^{\circ}$, (b) The f factor for the ^{48}Fe β decay normalized to unity at $E_x = 0$ MeV. (c) The modified ^{48}Ti(^{3}He ,t)^{48}V spectrum obtained by multiplying the spectrum in (a) with the f factor in (b). (d) The deduced β-decay spectrum ^{48}Mn after correcting for the IAS strength (see text), and (e) the same spectrum shown on a scale expanded by a factor of 10.

R^2 as explained in Sec. III, to predict the β-decay spectrum of ^{48}Fe $\rightarrow$ ^{48}Mn, on the assumption of isospin symmetry, which would mean that $T_z = \pm 2 \rightarrow \pm 1$ mirror GT transitions have the same values of B(GT). First, the phase-space (f) factor of β decay [45] for each transition was calculated using the Q_β [46] of the ^{48}Fe β decay, and the ^{48}Ti(^{3}He ,t) spectrum was multiplied by the f factor. Since the f factor is proportional to $(Q_\beta - E_x)^5$ [47] it decreases rapidly with E_x as shown in Fig. 7(b). In the ^{48}V nucleus the 3.018 MeV state is the IAS populated with the strength B(F) = 4 by a Fermi transition. The coupling constants for Fermi and GT transitions (governed by σ and $\sigma\tau$ operators, respectively) are different in the ^{48}Ti(^{3}He ,t)^{48}V reaction and ^{48}Fe β decay. Thus in predicting the β-decay spectrum the intensity of the IAS peak in Fig. 7(c) has to be increased by a factor of R^2/λ^2, that is $\approx$5.1. Here λ is the ratio between the axial-vector coupling constant and the vector coupling constant, $g_A/g_V = -1.270(3)$ [48]. Figure 7(d) shows the resulting β-decay spectrum expected to be observed in ^{48}Fe β decay. A detailed explanation of this procedure is given in Ref. [49]. This spectrum has recently been measured at LISE-GANIL [50]. It turns out that the measured spectrum is similar to that predicted in Fig. 7(d) but there are some discrepancies. In particular the 3864 keV 1^+ state populated in the CE experiment appears to correspond to three separate states when seen in β decay. The reasons for the differences are not yet understood and will be the subject of further study. The states corresponding to those at 2288 and 2406 keV lying below the IAS and populated in the CE reaction were not seen in the β decay of ^{48}Fe, presumably because of the background of β particles at lower energy in the spectrum.

V. SUMMARY

The $T_z = +2 \rightarrow +1$, GT transitions were studied in the ^{48}Ti(^{3}He ,t)^{48}V reaction at the intermediate beam energy of 140 MeV/nucleon and 0° scattering angle. An energy resolution of 21 keV was achieved. This was among the best energy resolutions that has ever been achieved at this incoming beam energy of 420 MeV. Owing to this excellent energy resolution many discrete states, including those weakly populated, could be studied up to 12.7 MeV. From the analysis of the angular distributions of the outgoing tritons it was possible to identify $\Delta L = 0$ transitions from their characteristic, forward-peaked angular distributions. The GT strength was found to be highly fragmented among many transitions. No strong concentration of the strength in the form of a GT resonance was observed. In addition, judging from the increasing trend of the accumulated sum of the B(GT) strength, it seems that strength still exists even in the region above 12 MeV.

Shell-model calculations were performed using the GXPF1J interaction. It was shown that the calculations reproduce the observed B(GT) strength reasonably well in the region up to 5 MeV but above this energy they exceed the measured values. It should be stressed that the study of GT transition strengths starting from an exotic nucleus, such as ^{48}Fe, contributes to the understanding of weak processes that are important in astrophysics and have not been well studied previously. The measured B(GT) distribution for the ^{48}Ti(^{3}He ,t)^{48}V reaction was compared with the corresponding measured distribution for the ^{47}Ti(^{3}He ,t)^{47}V reaction. The distributions follow roughly the same pattern but the latter is shifted to higher energies by about 2 MeV. A qualitative explanation is given in terms of the interactions of the particles involved and more specifically in terms of the transformation of the paired and unpaired valence particles. This explanation is corroborated by theory. On the assumption of isospin symmetry it is possible to use the measured B(GT) distribution in the ^{48}Ti(^{3}He ,t)^{48}V reaction to predict the distribution of B(GT) strength in the analogous β decay of the $T_z = -2$ nucleus ^{48}Fe.

ACKNOWLEDGMENTS

The authors thank the accelerator group of RCNP, Osaka, where the high-resolution (^{3}He ,t) experiment was performed under the experimental program No. E307, and Prof. R. Johnson (Surrey) for discussions. Y.F. acknowledges the support of MEXT, Japan, under Grants No. 22540310 and

No. 15K05104; E.G. the support of RCNP; B.R., A.A., and E.E.A. the support of the Spanish Ministry under Grants No. FPA2005-03993, No. FPA2008-06419-C02-01, No. FPA2011-24553, and No. FPA2014-52823-C2-1-P; and R.G.T.Z., J.D., C.J.G., R.M., and G.P. the support of US NSF under Grants No. PHY-0606007 and No. PHY-0822648(JINA). Y.F. and B.R. also acknowledge the support of the Japan-Spain collaboration program by JSPS and CSIC under the JSPS Bilateral Joint Projects/Seminars FY2011 programme.

[1] F. Osterfeld, Rev. Mod. Phys. **64**, 491 (1992), and references therein.
[2] J. Rapaport and E. Sugarbaker, Annu. Rev. Nucl. Part. Sci. **44**, 109 (1994).
[3] D. Frekers, Prog. Part. Nucl. Phys. **57**, 217 (2006).
[4] Y. Fujita, B. Rubio, and W. Gelletly, Prog. Part. Nucl. Phys. **66**, 549 (2011).
[5] A. L. Cole, H. Akimune, Sam M. Austin, D. Bazin, A. M. van den Berg, G. P. A. Berg, J. Brown, I. Daito, Y. Fujita, M. Fujiwara, S. Gupta, K. Hara, M. N. Harakeh, J. Jänecke, T. Kawabata, T. Nakamura, D. A. Roberts, B. M. Sherrill, M. Steiner, H. Ueno, and R. G. T. Zegers, Phys. Rev. C **74**, 034333 (2006).
[6] T. N. Taddeucci, C. A. Goulding, T. A. Carey, R. C. Byrd, C. D. Goodman, C. Gaarde, J. Larsen, D. Horen, J. Rapaport, and E. Sugarbaker, Nucl. Phys. A **469**, 125 (1987), and references therein.
[7] W. G. Love, K. Nakayama, and M. A. Franey, Phys. Rev. Lett. **59**, 1401 (1987).
[8] Y. Fujita, K. Hatanaka, G. P. A. Berg, K. Hosono, N. Matsuoka, S. Morinobu, T. Noro, M. Sato, K. Tamura, and H. Ueno, Nucl. Instrum. Methods Phys. Res. B **126**, 274 (1997), and references therein.
[9] http://www.rcnp.osaka-u.ac.jp.
[10] H. Fujita, Y. Fujita, T. Adachi, A. D. Bacher, G. P. A. Berg, T. Black, E. Caurier, C. C. Foster, H. Fujimura, K. Hara, K. Harada, K. Hatanaka, J. Jänecke, J. Kamiya, Y. Kanzaki, K. Katori, T. Kawabata, K. Langanke, G. Martìnez-Pinedo, T. Noro, D. A. Roberts, H. Sakaguchi, Y. Shimbara, T. Shinada, E. J. Stephenson, H. Ueno, T. Yamanaka, M. Yoshifuku, and M. Yosoi, Phys. Rev. C **75**, 034310 (2007).
[11] Y. Fujita, Y. Shimbara, I. Hamamoto, T. Adachi, G. P. A. Berg, H. Fujimura, H. Fujita, J. Görres, K. Hara, K. Hatanaka, J. Kamiya, T. Kawabata, Y. Kitamura, Y. Shimizu, M. Uchida, H. P. Yoshida, M. Yoshifuku, and M. Yosoi, Phys. Rev. C **66**, 044313 (2002).
[12] Y. Fujita, Y. Shimbara, A. F. Lisetskiy, T. Adachi, G. P. A. Berg, P. von Brentano, H. Fujimura, H. Fujita, K. Hatanaka, J. Kamiya, T. Kawabata, H. Nakada, K. Nakanishi, Y. Shimizu, M. Uchida, and M. Yosoi, Phys. Rev. C **67**, 064312 (2003).
[13] Y. Fujita, H. Akimune, I. Daito, H. Fujimura, M. Fujiwara, M. N. Harakeh, T. Inomata, J. Jänecke, K. Katori, A. Tamii, M. Tanaka, H. Ueno, and M. Yosoi, Phys. Rev. C **59**, 90 (1999).
[14] Y. Fujita, R. Neveling, H. Fujita, T. Adachi, N. T. Botha, K. Hatanaka, T. Kaneda, H. Matsubara, K. Nakanishi, Y. Sakemi, Y. Shimizu, F. D. Smit, A. Tamii, and M. Yosoi, Phys. Rev. C **75**, 057305 (2007).
[15] E. Ganioğlu, H. Fujita, Y. Fujita, T. Adachi, A. Algora, M. Csatlós, J. M. Deaven, E. Estevez-Aguado, C. J. Guess, J. Gulyás, K. Hatanaka, K. Hirota, M. Honma, D. Ishikawa, A. Krasznahorkay, H. Matsubara, R. Meharchand, F. Molina, H. Okamura, H. J. Ong, T. Otsuka, G. Perdikakis, B. Rubio, C. Scholl, Y. Shimbara, G. Susoy, T. Suzuki, A. Tamii, J. H. Thies, R. G. T. Zegers, and J. Zenihiro, Phys. Rev. C **87**, 014321 (2013).
[16] F. Molina, B. Rubio, Y. Fujita, W. Gelletly, J. Agramunt, A. Algora, J. Benlliure, P. Boutachkov, L. Caceres, R. B. Cakirli, E. Casarejos, C. Domingo-Pardo, P. Doornenbal, A. Gadea, E. Ganioğlu, M. Gascon, H. Geissel, J. Gerl, M. Gorska, J. Grebosz, R. Hoischen, R. Kumar, N. Kurz, I. Kojouharov, L. A. Susam, H. Matsubara, A. I. Morales, Y. Oktem, D. Pauwels, D. Perez-Loureiro, S. Pietri, Zs. Podolyak, W. Prokopowicz, D. Rudolph, H. Schaffner, S. J. Steer, J. L. Tain, A. Tamii, S. Tashenov, J. J. Valiente-Dobon, S. Verma, and H -J. Wollersheim, Phys. Rev. C **91**, 014301 (2015).
[17] R. G. T. Zegers, H. Akimune, Sam M. Austin, D. Bazin, A. M. van den Berg, G. P. A. Berg, B. A. Brown, J. Brown, A. L. Cole, I. Daito, Y. Fujita, M. Fujiwara, S. Galès, M. N. Harakeh, H. Hashimoto, R. Hayami, G. W. Hitt, M. E. Howard, M. Itoh, J. Jänecke, T. Kawabata, K. Kawase, M. Kinoshita, T. Nakamura, K. Nakanishi, S. Nakayama, S. Okumura, W. A. Richter, D. A. Roberts, B. M. Sherrill, Y. Shimbara, M. Steiner, M. Uchida, H. Ueno, T. Yamagata, and M. Yosoi, Phys. Rev. C **74**, 024309 (2006).
[18] T. Wakasa, K. Hatanaka, Y. Fujita, G. P. A. Berg, H. Fujimura, H. Fujita, M. Itoh, J. Kamiya, T. Kawabata, K. Nagayama, T. Noro, H. Sakaguchi, Y. Shimbara, H. Takeda, K. Tamura, H. Ueno, M. Uchida, M. Uraki, and M. Yosoi, Nucl. Instrum. Methods Phys. Res. A **482**, 79 (2002).
[19] M. Fujiwara, H. Akimune, I. Daito, H. Fujimura, Y. Fujita, K. Hatanaka, H. Ikegami, I. Katayama, K. Nagayama, N. Matsuoka, S. Morinobu, T. Noro, M. Yoshimura, H. Sakaguchi, Y. Sakemi, A. Tamii, and M. Yosoi, Nucl. Instrum. Methods Phys. Res. A **422**, 484 (1999).
[20] T. Noro *et al.*, RCNP Annual Report 1991 (Osaka Univ.), p.177 (unpublished).
[21] H. Fujita, Y. Fujita, G. P. A. Berg, A. D. Bacher, C. C. Foster, K. Hara, K. Hatanaka, T. Kawabata, T. Noro, H. Sakaguchi, Y. Shimbara, T. Shinada, E. J. Stephenson, H. Ueno, and M. Yosoi, Nucl. Instrum. Methods Phys. Res. A **484**, 17 (2002).
[22] Y. Fujita, H. Fujita, G. P. A. Berg, K. Harada, K. Hatanaka, T. Kawabata, T. Noro, H. Sakaguchi, T. Shinada, Y. Shimbara, T. Taki, H. Ueno, and M. Yosoi, J. Mass Spectrom. Soc. Jpn. **48(5)**, 306 (2000).
[23] H. Fujita, G. P. A. Berg, Y. Fujita, K. Hatanaka, T. Noro, E. J. Stephenson, C. C. Foster, H. Sakaguchi, M. Itoh, T. Taki, K. Tamura, and H. Ueno, Nucl. Instrum. Methods Phys. Res. A **469**, 55 (2001).
[24] T. Adachi, Y. Fujita, A. D. Bacher, G. P. A. Berg, T. Black, D. De Frenne, C. C. Foster, H. Fujita, K. Fujita, K. Hatanaka, M. Honma, E. Jacobs, J. Jänecke, K. Kanzaki, K. Katori, K. Nakanishi, A. Negret, T. Otsuka, L. Popescu, D. A. Roberts, Y. Sakemi, Y. Shimbara, Y. Shimizu, E. J. Stephenson, Y. Tameshige, A. Tamii, M. Uchida, H. Ueno, T. Yamanaka, M. Yosoi, and K. O. Zell, Phys. Rev. C **85**, 024308 (2012).

[25] T. W. Burrows, Nucl. Data Sheets **107**, 1747 (2006).
[26] A computer program SFIT, H. Fujita *et al.*, RCNP (Osaka University), Annual Report, 2010 (unpublished), p. 3.
[27] Y. Fujita, H. Fujita, T. Adachi, C. L. Bai, A. Algora, G. P. A. Berg, P. von Brentano, G. Coló, M. Csatlós, J. M. Deaven, E. Estevez-Aguado, C. Fransen, D. De Frenne, K. Fujita, E. Ganioğlu, C. J. Guess, J. Gulyás, K. Hatanaka, K. Hirota, M. Honma, D. Ishikawa, E. Jacobs, A. Krasznahorkay, H. Matsubara, K. Matsuyanagi, R. Meharchand, F. Molina, K. Muto, K. Nakanishi, A. Negret, H. Okamura, H. J. Ong, T. Otsuka, N. Pietralla, G. Perdikakis, L. Popescu, B. Rubio, H. Sagawa, P. Sarriguren, C. Scholl, Y. Shimbara, Y. Shimizu, G. Susoy, T. Suzuki, Y. Tameshige, A. Tamii, J. H. Thies, M. Uchida, T. Wakasa, M. Yosoi, R. G. T. Zegers, K. O. Zell, and J. Zenihiro, Phys. Rev. Lett. **112**, 112502 (2014).
[28] Y. Fujita, H. Fujita, T. Adachi, G. Susoy, A. Algora, C. L. Bai, G. Colò, M. Csatlós, J. M. Deaven, E. Estevez-Aguado, C. J. Guess, J. Gulyás, K. Hatanaka, K. Hirota, M. Honma, D. Ishikawa, A. Krasznahorkay, H. Matsubara, R. Meharchand, F. Molina, H. Nakada, H. Okamura, H. J. Ong, T. Otsuka, G. Perdikakis, B. Rubio, H. Sagawa, P. Sarriguren, C. Scholl, Y. Shimbara, E. J. Stephenson, T. Suzuki, A. Tamii, J. H. Thies, K. Yoshida, R. G. T. Zegers, and J. Zenihiro, Phys. Rev. C **91**, 064316 (2015).
[29] dw81, a DWBA computer code by J. R. Comfort (1981) used in an updated version (1986), an extended version of dwba70 by R. Schaeffer and J. Raynal (1970).
[30] S. Y. van der Werf, S. Brandenburg, P. Grasdijk, W. A. Sterrenburg, M. N. Harakeh, M. B. Greenfield, B. A. Brown, and M. Fujiwara, Nucl. Phys. A **496**, 305 (1989).
[31] R. Schaeffer, Nucl. Phys. A **164**, 145 (1971).
[32] R. G. T. Zegers, H. Abend, H. Akimune, A. M. van den Berg, H. Fujimura, H. Fujita, Y. Fujita, M. Fujiwara, S. Galès, K. Hara, M. N. Harakeh, T. Ishikawa, T. Kawabata, K. Kawase, T. Mibe, K. Nakanishi, S. Nakayama, H. Toyokawa, M. Uchida, T. Yamagata, K. Yamasaki, and M. Yosoi, Phys. Rev. Lett. **90**, 202501 (2003).
[33] J. Kamiya, K. Hatanaka, T. Adachi, K. Fujita, K. Hara, T. Kawabata, T. Noro, H. Sakaguchi, N. Sakamoto, Y. Sakemi, Y. Shimbara, Y. Shimizu, S. Terashima, M. Uchida, T. Wakasa, Y. Yasuda, H. P. Yoshida, and M. Yosoi, Phys. Rev. C **67**, 064612 (2003).
[34] Y. Fujita, J. Phys.: Conf. Ser. **20**, 107 (2005).
[35] T. Adachi, Y. Fujita, P. von Brentano, G. P. A. Berg, C. Fransen, D. De Frenne, H. Fujita, K. Fujita, K. Hatanaka, M. Honma, E. Jacobs, J. Kamiya, K. Kawase, T. Mizusaki, K. Nakanishi, A. Negret, T. Otsuka, N. Pietralla, L. Popescu, Y. Sakemi, Y. Shimbara, Y. Shimizu, Y. Tameshige, A. Tamii, M. Uchida, T. Wakasa, M. Yosoi, and K. O. Zell, Nucl. Phys. A **788**, 70 (2007).
[36] T. Adachi, Y. Fujita, P. von Brentano, A. F. Lisetskiy, G. P. A. Berg, C. Fransen, D. De Frenne, H. Fujita, K. Fujita, K. Hatanaka, M. Honma, E. Jacobs, J. Kamiya, K. Kawase, T. Mizusaki, K. Nakanishi, A. Negret, T. Otsuka, N. Pietralla, L. Popescu, Y. Sakemi, Y. Shimbara, Y. Shimizu, Y. Tameshige, A. Tamii, M. Uchida, T. Wakasa, M. Yosoi, and K. O. Zell, Phys. Rev. C **73**, 024311 (2006).
[37] L. Popescu, T. Adachi, G. P. A. Berg, P. von Brentano, D. Frekers, D. De Frenne, K. Fujita, Y. Fujita, E.-W. Grewe, M. N. Harakeh, K. Hatanaka, E. Jacobs, K. Nakanishi, A. Negret, Y. Sakemi, Y. Shimbara, Y. Shimizu, Y. Tameshige, A. Tamii, M. Uchida, H. J. Wörtche, and M. Yosoi, Phys. Rev. C **79**, 064312 (2009).
[38] Y. Fujita *et al.*, RCNP (Osaka University), Annual Report, 2010 (unpublished), p. 1.
[39] Y. Fujita *et al.*, RCNP (Osaka University), Annual Report, 2010 (unpublished), p. 2.
[40] M. Honma, T. Otsuka, B. A. Brown, and T. Mizusaki, Phys. Rev. C **69**, 034335 (2004).
[41] M. Honma, T. Otsuka, T. Mizusaki, M. Hjorth-Jensen, and B. A. Brown, J. Phys. Conf. Ser. **20**, 7 (2005).
[42] G. Martìnez-Pinedo, A. Poves, E. Caurier, and A. P. Zuker, Phys. Rev. C **53**, R2602 (1996).
[43] J. Jänecke, K. Pham, D. A. Roberts, D. Stewart, M. N. Harakeh, G. P. A. Berg, C. C. Foster, J. E. Lisantti, R. Sawafta, E. J. Stephenson, A. M. van den Berg, S. Y. van der Werf, S. E. Muraviev, and M. H. Urin, Phys. Rev. C **48**, 2828 (1993).
[44] Y. Shimbara, Y. Fujita, T. Adachi, G. P. A. Berg, H. Fujimura, H. Fujita, K. Fujita, K. Hara, K. Y. Hara, K. Hatanaka, J. Kamiya, K. Katori, T. Kawabata, K. Nakanishi, G. Martìnez-Pinedo, N. Sakamoto, Y. Sakemi, Y. Shimizu, Y. Tameshige, M. Uchida, M. Yoshifuku, and M. Yosoi, Phys. Rev. C **86**, 024312 (2012).
[45] N. B. Gove and M. J. Martin, Nucl. Data Tables **A10**, 246 (1971).
[46] M. Wang, G. Audi, A. H. Wapstra, F. G. Kondev, M. MacCormick, X. Xu, and B. Pfeiffer, Chin. Phys. C **36**, 1603 (2012).
[47] D. H. Wilkinson and B. E. F. Macefield, Nucl. Phys. A **232**, 58 (1974).
[48] J. C. Hardy and I. S. Towner, Nucl. Phys. News **16**, 11 (2006).
[49] Y. Fujita, T. Adachi, H. Fujita, A. Algora, B. Blank, M. Csatlós, J. M. Deaven, E. Estevez-Aguado, E. Ganioğlu, C. J. Guess, J. Gulyás, K. Hatanaka, K. Hirota, M. Honma, D. Ishikawa, A. Krasznahorkay, H. Matsubara, R. Meharchand, F. Molina, H. Okamura, H. J. Ong, T. Otsuka, G. Perdikakis, B. Rubio, C. Scholl, Y. Shimbara, E. J. Stephenson, G. Susoy, T. Suzuki, A. Tamii, J. H. Thies, R. G. T. Zegers, and J. Zenihiro, Phys. Rev. C **88**, 014308 (2013).
[50] S. E. A. Orrigo, B. Rubio, Y. Fujita, W. Gelletly, J. Agramunt, A. Algora, P. Ascher, B. Bilgier, B. Blank, L. Caceres, R. B. Cakirli, E. Ganioğlu, M. Gerbaux, J. Giovinazzo, S. Grevy, O. Kamalou, H. C. Kozer, L. Kucuk, T. Kurtukian-Nieto, F. Molina, L. Popescu, A. M. Rogers, G. Susoy, C. Stodel, T. Suzuki, A. Tamii, and J. C. Thomas, Phys. Rev. C **93**, 044336 (2016).